Conference materials
UDC 537.533.2
DOI: https://doi.org/10.18721/JPM.161.205

Methods for processing field emission glow patterns to obtain the I–V characteristics of individual emission sites

A.G. Kolosko [1]✉, S.V. Filippov [1], E.O. Popov [1]

[1] Ioffe Institute, St.-Petersburg, Russia

✉ agkolosko@mail.ru

Abstract. The work describes the features of processing glow patterns of the field emission projector when obtaining local I–V characteristics of individual emission sites. The features of constructing such dependencies are shown with the example of an experiment with a nanocomposite field emitter. The main factors influencing the analysis of glow patterns are discussed: the illumination effect, the halo effect, adsorption-desorption processes, vacuum discharges, burnout and contamination of the phosphor screen. Algorithms for reducing these effects with the computer processing of experimental data are described.

Keywords: field emission, emission glow patterns, local current-voltage characteristics

Citation: Kolosko A.G., Filippov S.V., Popov E.O., Methods for processing field emission glow patterns to obtain the I–V characteristics of individual emission sites, St. Petersburg State Polytechnical University Journal. Physics and Mathematics. 16 (1.2) (2023) 39–46. DOI: https://doi.org/10.18721/JPM.161.205

Материалы конференции
УДК 537.533.2
DOI: https://doi.org/10.18721/JPM.161.205

Методы обработки полевых эмиссионных картин свечения для получения I–V характеристик отдельных эмиссионных центров

А.Г. Колосько [1]✉, С.В. Филиппов [1], Е.О. Попов [1]

[1] Физико-технический институт им. А.Ф. Иоффе РАН, Санкт-Петербург, Россия

✉ agkolosko@mail.ru

Аннотация. В работе описаны особенности обработки картин свечения полевого эмиссионного проектора при получении локальных ВАХ отдельных эмиссионных центров. Особенности построения таких зависимостей показаны на примере эксперимента с нанокомпозитным полевым эмиттером. Обсуждаются основные факторы, влияющие на анализ картин свечения: эффект засветки, эффект гало, процессы адсорбции-десорбции, вакуумные разряды, выгорание и загрязнение люминофорного экрана. Описаны алгоритмы уменьшения этих эффектов с помощью компьютерной обработки экспериментальных данных.

Ключевые слова: полевая эмиссия, эмиссионные картины свечения, локальные вольт-амперные характеристики

Ссылка при цитировании: Колосько А.Г., Филиппов С.В., Попов Е.О. Методы обработки полевых эмиссионных картин свечения для получения ВАХ отдельных эмиссионных центров // Научно-технические ведомости СПбГПУ. Физико-математические науки. 2023. Т. 16. № 1.2. С. 39–46. DOI: https://doi.org/10.18721/JPM.161.205

Introduction

With the development of electronics and materials science in the field of nanoscale structures, vacuum electronics acquired new perspectives, which once gave way to solid-state semiconductor devices. The new vacuum nanoelectronics is capable of surpassing classical devices in terms of speed and reliability. The developed devices are based on sources of free electrons, which are multitip emission systems – LAFE (large area field emitters), in which the current load is distributed over an array of nanosized emitters. For the formation of sufficiently powerful and stable LAFE, a directed technological optimization is required. One of the options for such optimization is a detailed study of individual emission sites in the LAFE array.

There are several methods for obtaining the emission characteristics of individual emission sites: SAFEM (scanning anode with a hole) [1], STM (scanning with a tunneling microscope needle) [2], ILMS (analysis of the glow patterns of a field emission projector) [3]. The digital processing of glow patterns is based on the assumption that the brightness of the image of each emission site in the glow pattern is directly proportional to its current load. These brightnesses are used as weighting factors to calculate the corresponding local currents from the total emission current.

Usually, when observing individual emission sites, their field enhancement factor (FEF) is estimated at a fixed voltage level. However, the local current-voltage characteristic (IVC) has more complete information. It can be used to estimate not only FEF, but also the field emission area (FEA), as well as the dependence of these parameters on the voltage level.

Earlier in the ref. [4], we presented three methods for obtaining local emission characteristics using ILMS technique. The first method is based on processing the IVC in semi-logarithmic Fowler-Nordheim coordinates to obtain the effective FEF (γ_{eff}) and the effective FEA of one site ($S_1 = S_{eff} / N_{sites}$, where S_{eff} is the effective FEA of the entire cathode, N_{sites} is the number of sites) [5]. These two effective parameters are in some way an average of the actual emission characteristics of individual sites of the cathode surface.

The second method uses a fixed value of the emission area of one site (obtained, for example, by computer simulation [6]) and plots a histogram of the maximum emission currents of individual emission sites based on the processing of the glow patterns of the field projector at a constant voltage level. From these currents, the local FEFs are found.

The third method is based on a smooth change in the level of the applied voltage and continuous registration of local currents of all found emission sites (as mentioned above, the local currents are obtained by glow patterns processing). As a result, local IVCs are obtained. Further, these IVCs are processed in semi-logarithmic Fowler-Nordheim coordinates and the local FEF and FEA are estimated.

The construction of local IVCs encounters a number of difficulties in processing glow patterns. In this paper, we consider the features of obtaining local IVCs by the computerized ILMS technique with the example of experiments with a nanocomposite field cathode based on carbon nanotubes in a polystyrene (CNT/PS).

Experimental

To record experimental data, a complex technique for studying the properties of field emitters was used [7]. The experimental setup is a vacuum chamber (vacuum no worse than 10^{-7} Torr) with a plane-parallel system of electrodes, one of which has emission properties (in this work, this is a CNT/PS nanocomposite with a nanostructured surface). The voltage is applied in half-sine pulses, so that the emission current also has a pulsed character. During the experiment, IVCs are recorded one for every 20 ms (fast IVCs), as well as the time dependences of the amplitudes of the voltage and emission current pulses (I-V(t)). Registration is performed using a computerized system based on the NI DAQ PCIe-6351 multi-channel data acquisition board.

The distribution patterns of emission sites over the cathode surface (glow patterns) are recorded using a field projector system: the anode is made in the form of a transparent glass plate with an ITO layer coated with a phosphor. Patterns are registered using a long-focus USB microscope (Levenhuk DTX 90), which is located outside the vacuum chamber opposite the transparent window.

For registration and online data processing, we used a special multi-module program “Hephaestus” which is written on the LabVIEW graphical programming platform.

The software is equipped with modules that make it possible to continuously record voltage and current pulses, as well as the vacuum level, into a ".txt" file and simultaneously record glow patterns into an ".avi" file. A separate module "Morpheus" allows to repeatedly reproduce experiment data in the processor modules of "Hephaestus" in the passive experiment mode [8]. The use of this module makes it possible to study in detail and improve the software mechanism for obtaining information from the glow patterns in conjunction with the analysis of electrical characteristics (fast IVCs and I-V(t)).

Figure 1 shows the time dependences of the current, voltage and vacuum levels, as well as the averaged fast IVC, obtained during the experiment with the CNT/PS nanocomposite in the constant voltage mode (1 minute at 1.98 kV with current level 1 mA). This experiment is necessary to collect data on the emission surface before plotting local IVCs.

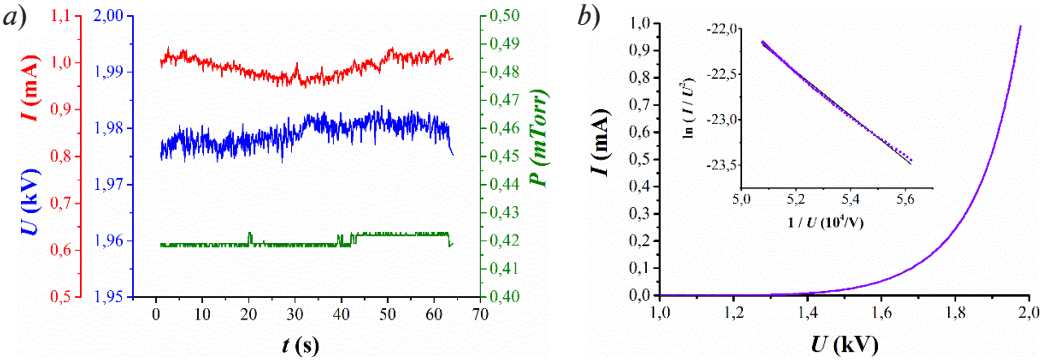

Fig. 1. Results of experiment with constant voltage level: time dependences of current, voltage and vacuum levels (*a*), averaged fast IVC and its analysis in the Fowler-Nordheim coordinates (*b*)

Estimation of the effective parameters of the cathode using IVC analysis in the classical Fowler-Nordheim coordinates gave the values $\gamma_{eff} = 979$ и $S_{eff} = 0.209$ μm².

Figure 2 shows the time dependences of the current, voltage, and vacuum levels, as well as the local IVC of the brightest site, obtained in the mode of a smoothly varying voltage level. Estimated values $\gamma_{local} = 1391$ и $S_{local} = 2.1$ nm².

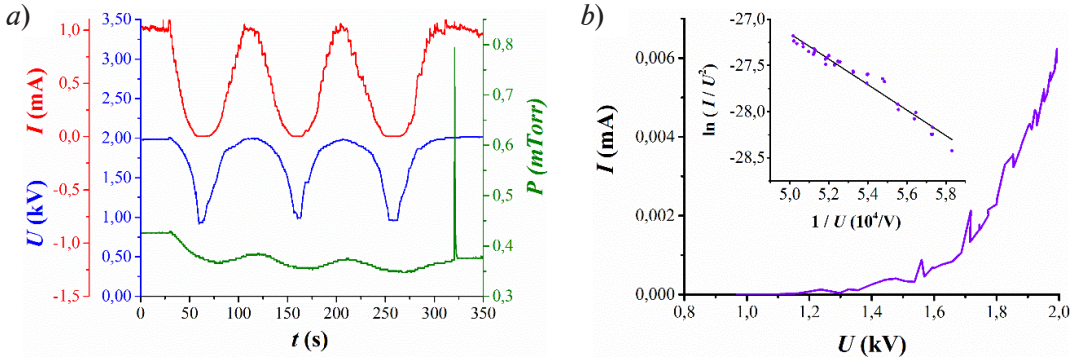

Fig. 2. Results of the experiment with a smoothly varying voltage level: time dependences of current, voltage and vacuum levels (*a*), local IVC of the brightest emission site (*b*)

Glow pattern analysis

A number of technical difficulties prevent obtaining adequate information about the emitter surface from the "glow pattern".

A. Overexposure effect

Overexposure effect is the effect of individual emission sites in the glow pattern exceeding the maximum brightness that a microscope can register. To control the appearance of an overexposure effect in the experiment, a module is built into the program for processing glow patterns, which converts the picture to gray tones online and builds a histogram of the distribution of pixels on the shades of gray (from 0 to 255). The overexposure effect appears as excess number of pixels at the edge of the range (Fig. 3, *a*). To eliminate this effect, a light filter is installed between the microscope and the window of the vacuum chamber. Note that the use of a light filter practically removes from

the glow pattern the dimmest emission sites (reduces them to the noise level), which can make a significant contribution to the total emission current.

Note that similar histograms are sometimes used by experimenters to estimate numerically the quality of the distribution of emission sites over the cathode surface [9]. On the other hand, the overexposure effect can be used to determine the FEA of an emission site (given as an overexposure area) [10], however, the correlation of this emission area with classical definitions raises many questions.

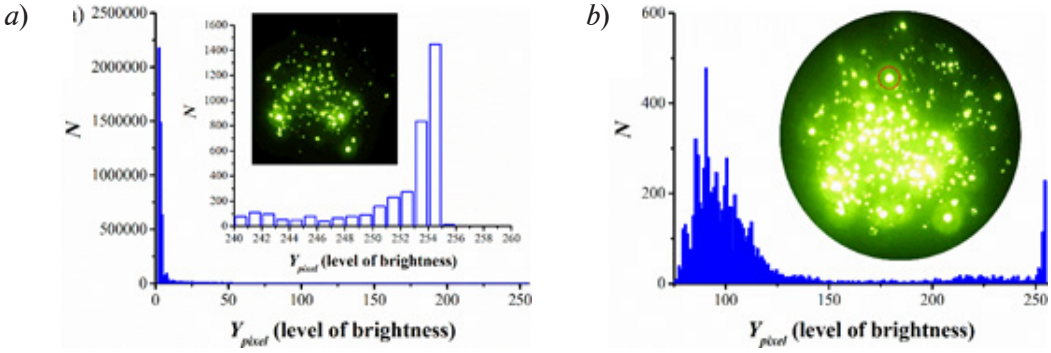

Fig. 3. Parasitic effects in glow patterns: pixel distribution histogram at the overexposure effect (*a*), pixel distribution histogram in a halo ring (*b*)

B. Scattering of electrons

The movement of electrons from the emission site to the anode is not linear: they move slightly at an angle and still repel each other in flight. Therefore, the site images are somewhat blurred [11]. The center of the emission site image (position with the maximum brightness) can be considered sufficiently reliable, because of electrons in this place fly along the shortest trajectory. The program "Hephaestus" searches for maxima in the glow pattern using a 3×3 pixels window, displays them on a black-and-white diagram in the form of white spots and highlights them with rectangular zones (the so-called ROI). In the Fig. 4, *a*, these zones are superimposed on the glow pattern.

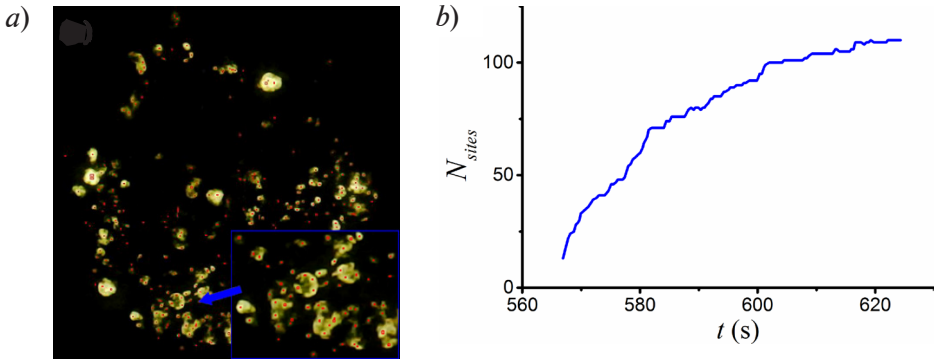

Fig. 4. Collection of information on the emission sites position on the cathode surface: finding emission sites in one frame of the glow pattern (*a*), time dependence of the number of emission sites found (*b*)

Further, the program monitors the detected zones and continuously searches for the pixels with maximum brightness $Y^{i}_{\max}$ in them. This brightness values are used as a weighting factors for distributing the total emission current to the individual emission sites. A smooth increase in the overall voltage level makes it possible to build a local IVC for each of emission site.

Note that the application of pattern filtering (in fact, its smoothing) makes it possible to eliminate digital noise from the search for brightness maxima. The program "Hephaestus" uses the Gaussian Kernels filter (a tool called IMAQ GetKernel VI). Details of the processing are described in [12].

C. Fluctuations of adsorbates

The second problem in the analysis of glow patterns is the instability in time. Some effects, which we consider below, can shift the position of the maximum brightness of the emission sites. However, the strongest influence on the stability is exerted by adsorption-desorption processes, which significantly change the work function of individual emission sites, causing them to practically disappear from the

glow pattern and then reappear. This leads to the fact that each frame with the glow pattern coming from the microscope must be processed for search a new set of emission sites. At the online data processing mode, this significantly slows down the analyze of the cathode surface, and also makes it impossible to build the time dependences of the local currents of the individual emission sites.

The solution to this problem is to follow the cathode surface for some time in order to find the positions of all (or at least the main) flickering sites. The "Hephaestus" program finds the positions of the sites by adding new positions of the brightness maxima to the overall black-and-white diagram. Each white spot in this diagram corresponds to the fluctuation region of one emission site. In the process of accumulation, the program builds a time dependence of the number of spots. When this curve reaches a relatively constant level, the collection of sites can be considered complete (Fig. 3, *b*).

This method has disadvantages: at a high density of sites, the effect of merging their spots on the black-and-white diagram occurs, as well as the effect of overlapping their resulting rectangular ROI (the program even has a built-in module for estimating the number and area of such ROI). The influence of these effects decreases with a decrease in the emission current level, as well as with the installation of a stronger light filter. Also, the effect is leveled by raising the threshold brightness level Y_{th}. In all three cases, dim sites are excluded (lost) from the analysis.

D. Galo effect

Another factor is the inability to distinguish the least bright emission sites from digital noise (pixel-sized bright dots) and from halo-type glows. Halo effects can be caused by the presence of parasitic conductive protrusions in the emission system (on the anode surface), which pull the electron flow towards themselves [11], as well as by the emission of secondary electrons from the anode surface, which scatter to the sides and bombard the phosphor away from the main electron flow, creating glowing rings in the pattern [14]. These glowing reflections are superimposed on the images of emission sites, blur these images, shift them to the side, and so change the brightness level. Moreover, due to halo effects, false peaks of brightness appear in the pattern (usually they located in the glowing rings around the sites images).

This effect can be neutralized by adding a current-carrying grid (the third electrode) to the system, located near the anode [15]. However, this grid will distort the emission pattern and may even lead to spurious diffraction effects if the grid cell size and the interelectrode spacing satisfy the diffraction conditions. Another variant is to use a phosphor with a low secondary emission coefficient [15].

Counteracting the appearance of spurious glows with the computer processing of glow patterns can be carried out in a rather complicated way: by searching for a symmetrical brightness profile of the brightest sites and subtracting the corresponding nonlinear correction from the pattern (Fig. 3, *b* shows the distribution of pixels in a halo-type ring, which has a customary asymmetric peak).

A simpler approach is to cut off the area of the pattern corresponding the cathode surface using a mask, as well as setting the threshold brightness Y_{th}, below which pixels should be excluded from the analysis. On the other hand, the application of the technique of virtual repeated experiment allows to create a certain pattern of threshold brightness (each pixel of the pattern has its own Y_{th}). Application of this threshold brightness pattern can include in the analysis fainter sites, which were previously excluded due to the influence of halo effects at the region of bright sites.

Fig. 5 shows the found sets of emission sites for direct processing of glow patterns, for pattern processing with Gaussian Kernels filter, and for processing with the filter and the threshold brightness pattern. Fig. 5, *a* – 764 sites, too many into each glowing spot at the pattern. Fig. 5, *b* – 138 sites, only the brightest. Fig. 5, *c* – 409 sites including dim sites. Corresponding current-voltage characteristics of this experiment are presented in Fig. 1.

E. Microscope and luminophore resolution

The resolution of the microscope matrix limits the resolution of the emission projector. Dividing the cathode diameter D_C (in our experiments, the metal substrate of the nanocomposite has a diameter of 1 cm) by the number of pixels in the diameter of corresponding cathode surface image N_p ("Hephaestus" determined it automatically by the mask size) gives size of pixel D_p. Microscope Levenhuk DTX 90 (matrix 2592 × 1944, 5 Mp) in our measuring system allows us to obtain $D_p = D_C / N_p \sim 10$ μm per pixel. That is, one luminous pixel can image a number of individual carbon nanotubes. Increasing the resolution of the microscope leads to an increase in the amount of data and to a slowdown in the speed of online processing, which is quite critical when constructing local IVCs.

The phosphor coating usually consists of grains of powder, which is applied to the anode surface in the suspension form. The size of these grains, as well as the resolution of the matrix, limits the

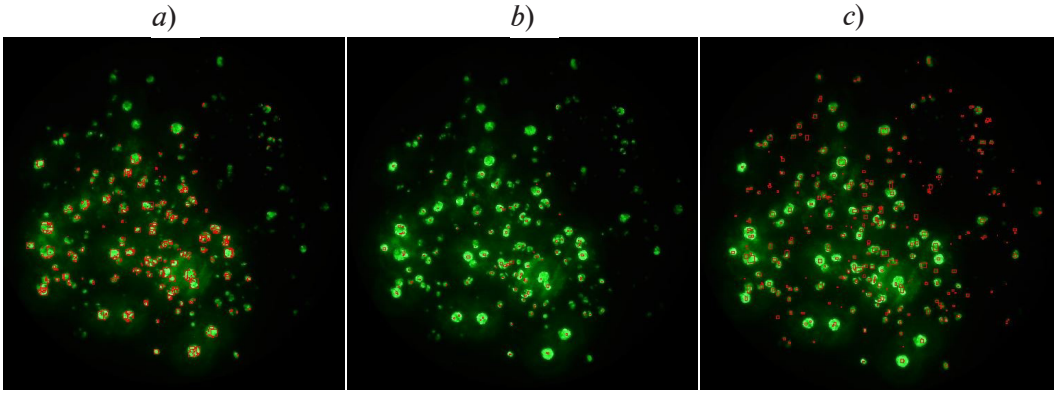

Fig. 5. Sets of emission sites obtained at: direct processing with threshold brightness Y_{th} = 150 (*a*), processing with Gaussian Kernels filter (10 times for each frame) (*b*), processing with the filter and the threshold brightness pattern ($\max Y_{th}$ = 150, $\min Y_{th}$ = 50 for the summary filtered pattern) (*c*)

resolution of the field emission projector. In our experiment, the grain size is less than 5 μm, that is comparable to the size of a pixel. At a sufficiently high density of the emission sites (the density generally increases with the applied voltage), they become indistinguishable, since the distance between sites becomes smaller than the phosphor grain [16].

The non-uniformity of the phosphor coating can also lead to an error in the calculations of the emission sites current load and, accordingly, to the incorrect building of local IVCs. This irregularity can result from local burning of the phosphor by electron beams of sufficiently high power, as well as from the transfer of particles from the cathode to the anode, which is especially often observed in experiments with a fresh emitter (the so-called high-voltage training of the emission surface).

On the other hand, the surface of the nanocomposite emitter is rough and may have macroscopic protrusions, on top of which there may be several emission sites (nanoemitters). A fairly close location of these sites can lead to the fact that in the glow pattern they will be represented by one spot with a common glow halo ring around this spot (Fig. 6, *a*). It is difficult to separate these sites inside this spot using a field projector (some of them merge into one spot in the black-and-white diagram), therefore, from an experimental point of view, it is advantageous to represent them as a single emission site with an increased FEA and an average FEF.

In the case of a sufficiently large distance between the emission sites on a common macroscopic ledge (so that even the halo glow around them is not round), they can be quite clearly separated from each other by the software processing (Fig. 6, *b*).

Note that there is an alternative to phosphor powders – luminescent crystals, for example YAG. However, just like powder, it is subject to the influence of electron bombardment and can degrade over time [17].

It is also worth mentioning the nonlinearity of the dependence of the phosphor brightness on the emission current $Y(I)$ (Fig. 6, *c*). In general, the dependence of the phosphor brightness on the current can have both a concave and a convex form [18]. This nonlinearity must be taken into account when comparing sets of emission sites and their corresponding local characteristics obtained at different current levels. It is possible to change the threshold brightness Y_{th} according to the empirical curve $Y(I)$.

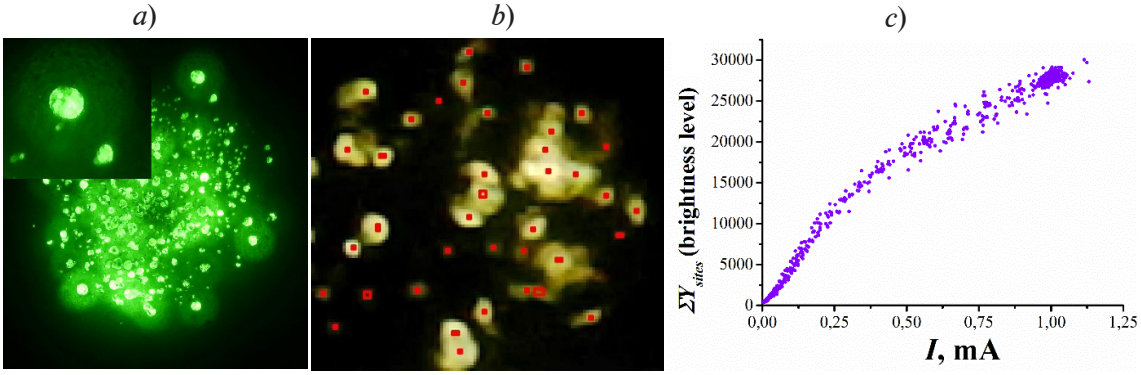

Fig. 6. Parasitic effects in the glow patterns: phosphor inhomogeneity (*a*), finding the emission sites position (*b*), dependence of the total emission current on the total brightness of the emission sites (*c*)

F. Irreversible processes

Another variant of changing the structure of the emission sites can be irreversible changes in the cathode surface under the influence of such factors as the pulling forces of the electric field [19] or microscopic vacuum discharges, which can both destroy the longest sites and generate new ones, deforming the surface.

Long-term observation of the nanocomposite cathode surface shows that new sites appear during the entire experiment. In this case, the analysis of glow patterns should be performed in the mode of a repeated virtual experiment, which is provided to the experimenter by the Morpheus software module described above. For the first pass, one can find the position of all sites, and on the next – to analyze their properties.

Conclusion

We have considered the features of processing glow patterns of the computerized field projector. Today, the world's leading laboratories that study field emission are equipped with such projectors made in USA [11, 17], Brazil [3], and Germany [20]. The main task is to obtain local emission characteristics of a multipoint field cathode and study its relationship with the features of macroscopic emission characteristics. Knowing the relationship between the shape and location of an individual emission sites in the common array of a multi-tip field cathode and the characteristics of the emission current (magnitude and stability) allows targeted optimization of the cathode surface. Optimization is necessary to obtain competitive devices for vacuum nanoelectronics, which already today exceed semiconductor analogues in terms of inertia, radiation resistance and energy efficiency.

REFERENCES

1. **Nilsson L., Groening O., Groening P., Kuettel O., Schlapbach L.,** Characterization of thin film electron emitters by scanning anode field emission microscopy, Journal of Applied Physics. 90 (2) (2001) 768–780.

2. **Xu Z., Bai X.D., Wang E.G., Wang Z.L.,** Field emission of individual carbon nanotube with in situ tip image and real work function, Applied Physics Letters. 87 (16) (2005) 163106-1–3.

3. **Kopelvski M.M., Ramirez-Fernandez F.J., Galeazzo E., Dantas M.O.S., Peres H.E.M.,** Potentialities of a new dedicated system for real time field emission devices characterization: a case study, 4th International Symposium on Instrumentation Systems, Circuits and Transducers (INSCIT), At Sro Paulo, Brazil, august (2019) 1–5.

4. **Popov E.O., Kolosko A.G., Filippov S.V., Ponyaev S.A.,** Methods for measuring the local emission characteristics of CNT based multi-tip emitters, Journal of Physics: Conference Series. 2103 (1) (2021) 012116-1–6.

5. **Popov E.O., Kolosko A.G., Filippov S.V.,** A Test for Compliance with the Cold Field Emission Regime Using the Elinson–Schrednik and Forbes–Deane Approximations (Murphy–Good Plot), Technical Physics Letters. 46 (9) (2020) 838–842.

6. **de Assis T.A., Dall'Agnol F.F., Andrade R.F.S.,** The consequences of dependence between the formal area efficiency and the macroscopic electric field on linearity behavior in Fowler–Nordheim plots, Journal of Physics D: Applied Physics. 49 (2016) 355301-1–11.

7. **Popov E.O., Kolosko A.G., Filippov S.V., Terukov E.I., Ryazanov R.M., Kitsyuk E.P.,** Comparison of macroscopic and microscopic emission characteristics of large area field emitters based on carbon nanotubes and graphene, Journal of Vacuum Science & Technology B, Nanotechnology and Microelectronics: Materials, Processing, Measurement, and Phenomena. 38 (4) (2020) 043203-1–10.

8. **Kolosko A.G., Chernova V.S., Filippov S.V., Popov E.O.,** Method for Recording and Reproducing an Experimental Research into the Field Emitter Properties Based on Carbon Nanotubes, Advanced Materials and Technologies. 3 (2020) 18–27.

9. **Fursey G.N., Novikov D.V., Dyuzhev G.A., Kotcheryzhenkov A.V., Vassiliev P.O.,** The field emission from carbon nanotubes, Applied surface science. 215 (1-4) (2003) 135–140.

10. **Patra R., Singh A., Vankar V. D., Ghosh S.,** Field emission image analysis: Precise determination of emission site density and other parameters, Advanced Materials Letters. 7 (10) (2016) 771–776.

11. **Fursey G.N.,** Field emission, Soros Educational Journal. 6 (11) (2000) 96–103.

12. **Filippov S.V., Popov E.O., Kolosko A.G., Vinnichek R.N.,** Evaluation of numerical characteristics

of the current load distribution on the surface of multi-tip field emitters, Journal of Physics: Conference Series. 917 (9) (2017) 092022-1–6.

13. **Posos T.Y., Fairchild S.B., Park J., Baryshev S.V.,** Field emission microscopy of carbon nanotube fibers: Evaluating and interpreting spatial emission, Journal of Vacuum Science & Technology B, Nanotechnology and Microelectronics: Materials, Processing, Measurement, and Phenomena. 38 (2) (2020) 024006-1–6.

14. **Nikolski K.N., Baturin A.S., Knyazev A.I., Tchesov R.G., Sheshin E.P.,** Formation of Rings around a Field-Emission Image and Possible Applications of This Effect, Technical Physics. 49 (2) (2004) 250–253.

15. **Il'ichev E.A., Kuleshov A.E., Petrukhin G.N., Minakov P.V., Rychkov G.S., Sen V.V., Teverovskaya E.G.,** Diamond Photocathodes As Field-Emission Electrodes for Vacuum Microelectronics, Technical Physics Letters. 47 (7) (2021) 503–506.

16. **Lyashenko S.A., Volkov A.P., Ismagilov R.R., Obraztsov A.N.,** Field electron emission from nanodiamond, Technical Physics Letters. 35 (3) (2009) 249–252.

17. **Baturin S.S., Baryshev S.V.,** Electron emission projection imager, Review of Scientific Instruments. 88 (3) (2017) 033701-1–7.

18. **Ozol D., Eliseev A., Garkusha M., Pavlenko A.,** Measurement Method of the Distribution of Field Emission Current, 2019 International Vacuum Electronics Conference (IVEC), april (2019) 1–2.

19. **Jung H., An S.Y., Jang D. M., Kim J. M., Park J. Y., Kim D.,** A multi-wall carbon nanotube/ polymethyl methacrylate composite for use in field emitters on flexible substrates, Carbon. 50 (3) (2012) 987–993.

20. **Serbun P., Porshyn V., Müller G., Lützenkirchen-Hecht D.,** Advanced field emission measurement techniques for research on modern cold cathode materials and their applications for transmission-type X-ray sources, Review of Scientific Instruments. 91 (8) (2020) 083906-1–19.

THE AUTHORS

KOLOSKO Anatoly G.
agkolosko@mail.ru
ORCID: 0000-0002-6073-6808

POPOV Eugeni O.
e.popov@mail.ioffe.ru
ORCID: 0000-0003-2226-6304

FILIPPOV Sergey V.
s.filippov@mail.ioffe.ru
ORCID: 0000-0001-5325-2226

Received 27.10.2022. Approved after reviewing 11.12.2022. Accepted 12.12.2022.